P-ISSN : 2598-1277
E-ISSN : 2621-3966

JOURNAL OF GREEN SCIENCE AND TECHNOLOGY

STRUCTURAL ANALYSIS OF 40-METER AND 50-METER SPAN ARAMCO CSP BRIDGES USING THE FINITE ELEMENT METHOD

Yulianto Bastian Zai[1], Pio Ranap Tua Naibaho[1*]

[1] Civil Engineering Program, Tama Jagakarsa University, Jakarta.
Corresponding Author's Email: pioranaptua@jagakarsa.ac.id
Corresponding Author's Phone Number: 081219114867

ABSTRACT

Corrugated Steel Structure (CSS) represents an alternative structural system that offers distinct advantages in terms of construction speed and material efficiency. This study aims to analyze the structural performance of long-span Aramco CSP bridges, specifically with 40-meter and 50-meter spans, using the Finite Element Method (FEM). The analysis refers to applicable bridge standards, while parameters not yet regulated in the Indonesian National Standard (SNI) are determined based on scientific references, international standards, and prior research. The analytical results indicate that the 40-meter span Aramco CSP bridge featuring a 13 mm Corrugated Steel Plate (CSP) with SS400 material grade experiences a maximum deflection of 12.438 mm, which is well below the allowable deflection limit of 50 mm. Meanwhile, the 50-meter span bridge with a 15 mm CSP thickness and SS490 material grade exhibits a maximum deflection of 22.350 mm, also below the allowable limit of 62.5 mm. From a mechanical perspective, this demonstrates that the arch configuration allows loads to be transferred via axial compressive forces toward the supports, thereby reducing bending moments within the structural elements. Consequently, this mechanism minimizes deflection and yields a more efficient internal force distribution. Equivalent stress analysis (Von Mises) reveals that the 40-meter span bridge generates a maximum stress of 310.33 MPa, which exceeds the material's yield strength of 250 MPa. In contrast, the 50-meter span bridge produces a maximum stress of 283.76 MPa, which remains below the material's yield strength of 285 MPa. Therefore, the 40-meter span Aramco CSP bridge requires structural reinforcement by either increasing the plate thickness or upgrading the material grade to fulfill the structural design criteria. The loads acting on the arch structure are propagated via axial compressive forces along the geometry toward both supports, effectively reducing bending stresses and resulting in minor deflections.

Keywords: Aramco, corrugated steel plate, corrugated steel structure, FEM.

1. INTRODUCTION

The concept of corrugation originally emerged to enhance the stiffness of thin metal sheets without significantly increasing their thickness, which would otherwise add substantial weight. A pivotal figure in developing this concept was James H. Watson. In 1896, Watson patented the corrugated steel structure system with a more systematic approach to evaluating structural capacities, specifically in compression and bending. In Indonesia, Aramco with an SS400 steel grade is commonly utilized as a structural material for bridge systems employing Corrugated Steel Structures (CSS). SS400 (Structural Steel) is a low-carbon steel manufactured via the hot-rolled method in compliance with the JIS G3101 standard, featuring a tensile strength ranging from 400 to 510 MPa and a yield strength of approximately 250 MPa. To date, the types of corrugated steel structures developed in Indonesia as primary components for flyovers and bridges include the Standard type (spans ranging from 6 m to 9 m), the Deep type (spans ranging from 24 m to 27 m), and the Excor type (spans ranging from 32 m to 35 m).

These current implementations indicate that the bridge lengths constructed using the CSS system are still classified as short-span structures (with a maximum length of 35 m). Consequently, this research is conducted to investigate longer 40-meter and 50-meter spans evaluated using the Finite Element Method (FEM) to analyze the resulting total deflection and Von Mises equivalent stress. Entering the 20th century, Corrugated Steel Structures began to be implemented in arch configurations. Arch systems and geometries are highly efficient due to their capability to predominantly transfer loads as compressive forces along the structural curvature. In contrast to conventional beams or girders that are predominantly subjected to bending, arch structures channel internal forces along their geometric path toward the supports. This mechanism drastically reduces the occurring bending moments, thereby optimizing material utilization and enhancing structural efficiency [1]. A Corrugated Steel Structure (CSS) refers to a type of construction component fabricated from steel plates that have been formed or bent into a repetitive corrugated pattern. This geometric configuration significantly increases the material's strength-to-stiffness ratio compared to flat sheets, thereby enabling it to support heavy loads while remaining relatively lightweight [2]. The Shamal Bridge in Dubai, United Arab Emirates (UAE), successfully established a Guinness World Record as a CSS bridge with a span reaching 32.39 meters utilizing a soil-steel bridge system. Within this system, the engineered backfill acts not only as a dead load but also functions as an integral part of the load-bearing system.

The interaction between the soil medium and the steel shell ensures a more uniform pressure distribution and helps enhance the structural capacity of the CSP [3]. The principle of soil-steel interaction is the core concept in Corrugated Steel Structures (CSS), utilizing a composite system between the engineered backfill and the corrugated steel plates. The backfill medium functions as a medium for load transfer and distribution, whereas the corrugated steel plate acts as a flexible element subjected to compressive forces [4]. According to [3], the arch model in CSS functions as a flexible structure that heavily relies on the interaction between the corrugated steel plates and the surrounding backfill material. The composite principle in Aramco CSP bridges involves a simultaneous interaction among the corrugated steel sheets, the engineered backfill, and the reinforced concrete structure. The flexible corrugated steel plates experience minor deformations when subjected to loads, which then triggers the surrounding specialized backfill to provide passive earth pressure that helps resist further deformation. This combination yields a more uniform stress redistribution and subsequently enhances the overall structural capacity [5].

The Finite Element Method (FEM) approach is critical in analyzing the structural behavior of corrugated steel plates, given that the cross-sectional geometry of corrugated plates generates complex mechanical behaviors, particularly due to geometric nonlinearity effects, local buckling, and soil-structure interaction [6]. The concepts of tensile and compressive stresses form the foundation for material mechanics analysis and structural material evaluation using the finite element method. This aligns with the study conducted by [7], which states that normal stress induces material deformation. Furthermore, finite element method (FEM) analysis serves as the primary approach for evaluating the structural behavior of Corrugated Steel Structure (CSS) bridges. The distribution of vehicular loads on CSS structures acts not only in the transverse direction but also propagates longitudinally, adhering to the orthotropic behavior of the corrugated plates [8]. In structural behavior analysis, evaluating stress and strain is a critical aspect of assessing the response of structural elements to loading conditions. The stress distribution developing within critical zones will influence strain patterns, crack initiation, stiffness degradation, and ultimately, structural failure mechanisms [9]. A nonlinear 3D FEM approach enables a more realistic modeling of structural behavior due to its capability to capture material nonlinearity, geometric nonlinearity, component contact interactions, plasticity, and buckling behaviors. This approach is highly effective for analyzing complex connections, nonlinear structures, and element joints [10].

2. RESEARCH METHOD

The research begins with a literature study to review corrugated steel structures (CSS), corrugated steel plates (CSP), Aramco bridges, the finite element method, and relevant supporting theories. References were gathered from books, scientific journals, catalogs, standards, and regulations concerning steel structures and bridges. Subsequently, structural analysis was conducted using

P-ISSN : 2598-1277
E-ISSN : 2621-3966

ANSYS Workbench, encompassing geometric modeling, material property definition, application of boundary conditions and loading specifications, and the mesh generation process. The analytical results, consisting of stress distributions and deflections, were then evaluated to determine the structural behavior under loading conditions.

Given that the implementation of long-span Aramco CSP bridges in Indonesia remains limited, the analysis refers to applicable national bridge standards. Parameters not yet regulated within the Indonesian National Standard (SNI) were determined based on scientific references, relevant international standards, and findings from prior research to ensure a justifiable technical foundation. The data collection process was conducted systematically to ensure high levels of validity and reliability, thereby maintaining scientific accountability [11]. According to ASTM A796/A796M-15A, corrugated steel plates (CSP) possess specific mechanical and sectional properties applicable to structural analysis and design. Consequently, mechanical data and section properties serve as an essential foundation in the design, analysis, and performance evaluation of corrugated steel structures [12]. In this study, the 40-meter span Aramco CSP bridge utilizes an SS400 material grade with a yield strength of 250 MPa, a tensile strength of 400 MPa, a profile thickness of 13 mm, and a crown height of 11 meters. The schematic cross-section of the 40-meter span Aramco CSP bridge is illustrated in the following figure.

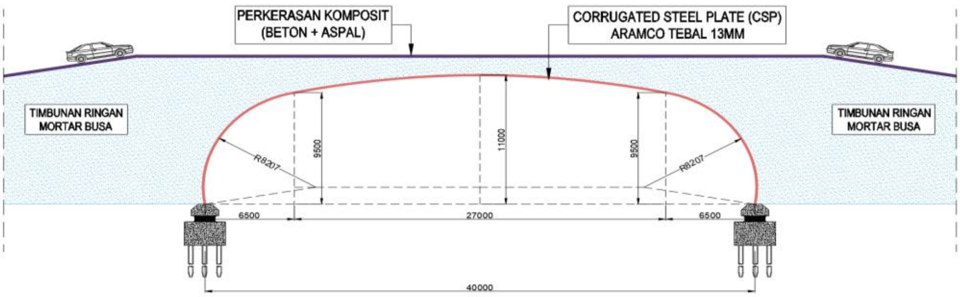

Figure 1. Schematic Cross-Section of the 40-Meter Span Aramco CSP Bridge

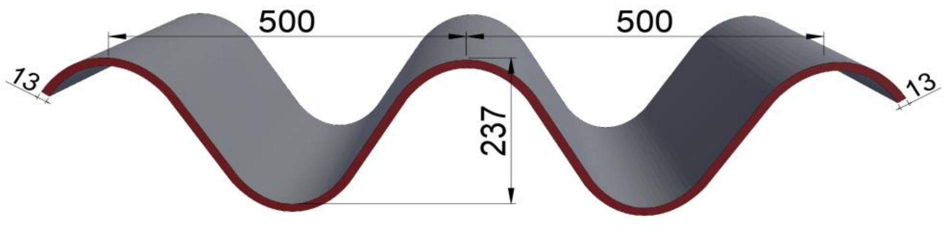

Figure 2. Steel Thickness Profile of the 40-Meter Span Aramco CSP Bridge

The 50-meter span Aramco CSP bridge utilizes an SS490 material grade with a yield strength of 285 MPa, a tensile strength of 490 MPa, a profile thickness of 15 mm, and a crown height of 12 meters.

P-ISSN : 2598-1277
E-ISSN : 2621-3966

The schematic cross-section of the 50-meter span Aramco CSP bridge is illustrated in the following figure.

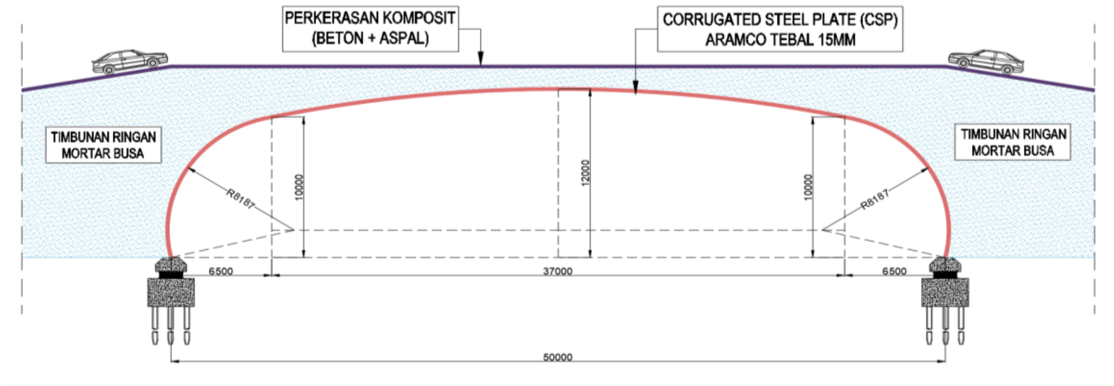

Figure 3. Schematic Cross-Section of the 50-Meter Span Aramco CSP Bridge

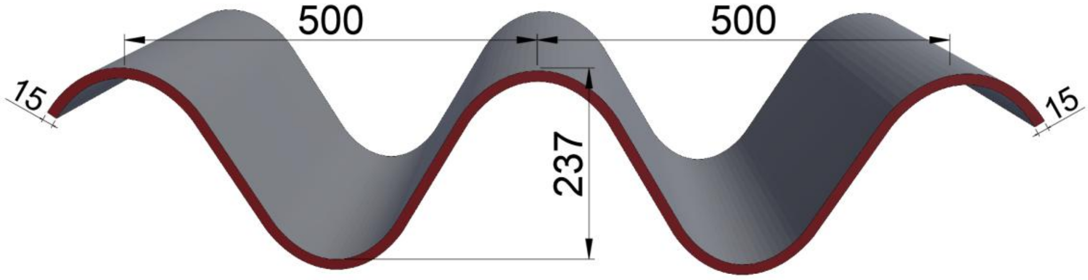

Figure 4. Steel Thickness Profile of the 50-Meter Span Aramco CSP Bridge

Both Aramco CSP bridge configurations feature a width of 10 meters, accommodating a two-lane two-way traffic system, 0.80-meter-wide sidewalks/shoulders on each side, and a 0.50-meter-wide median. The Aramco CSP steel structure is backfilled with lightweight foamed mortar and overlaid with a concrete rigid pavement. The applied loading specifications comply with SNI 1725:2016 and SNI 2833:2016.

Table 1. Applied Loads on the 40-Meter Span Aramco CSP Bridge Structure

Load Type	Value	Unit
Additional dead load (MA)	1,100.000	Pa
Uniformly distributed load (BTR / UDL)	7,850.000	Pa
Knife-edge load (BGT / KEL)	68,600.000	N/m
Pedestrian load (TP)	5,000.000	Pa
Braking force (TB)	181,500.000	N
Wind load on structure – windward (EWS Windward)	2,160.000	N/m
Wind load on structure – leeward (EWS Leeward)	1,080.000	N/m
Wind load on vehicles (EWL)	1,502.000	N/m
Uniform temperature load (EUN)	27.500	°C
Seismic load in x-direction (EQX)	624.850	N
Seismic load in y-direction (EQY)	624.850	N

Source: Author's Analysis, 2026

P-ISSN : 2598-1277
E-ISSN : 2621-3966

Table 2. Applied Loads on the 50-Meter Span Aramco CSP Bridge Structure

Load Type	Value	Unit
Additional dead load (MA)	1,100.000	Pa
Uniformly distributed load (BTR / UDL)	7,200.000	Pa
Knife-edge load (BGT / KEL)	68,600.000	N/m
Pedestrian load (TP)	5,000.000	Pa
Braking force (TB)	204,500.000	N
Wind load on structure – windward (EWS windward)	2,160.000	N/m
Wind load on structure – leeward (EWS leeward)	1,080.000	N/m
Wind load on vehicles (EWL)	1,502.000	N/m
Uniform temperature load (EUN)	27.500	°C
Seismic load in x-direction (EQX)	532.616	N
Seismic load in y-direction (EQY)	532.616	N

Source: Author's Analysis, 2026

Due to the limited implementation of long-span Aramco CSP bridges in Indonesia, the analysis strictly adheres to applicable national bridge standards, particularly the relevant SNIs. For design parameters that are not yet regulated or available within the SNI framework, engineering assumptions are established based on scientific references, international standards, and findings from prior literature. This approach is implemented to ensure that the geometric modeling and simulation procedures remain consistent, realistic, and technically justifiable, thereby enabling the analytical findings to serve as a reliable reference for evaluating the structural behavior of long-span Aramco CSP bridges regarding their induced deflections and stresses.

Table 3. Load Combinations

Limit State	***MS***	***MA***	***TD TB TP***	***EWs***	***EWL***	***EUn***	***EQ***
Strength I	1.0	1.4	1.8	-	-	1.2	-
Strength II	1.0	1.4	1.4	-	-	1.2	-
Strength III	1.0	1.4	-	1.4	-	1.2	-
Strength IV	1.0	1.4	-	-	-	1.2	-
Strength V	1.0	1.4	-	0.4	1.0	1.2	-
Extreme Event I	1.0	1.4	0.3	-	-	-	1.0
Extreme Event II	1.0	1.4	0.5	-	-	-	-
Service I	1.0	1.0	1.0	0.3	1.0	1.2	-
Service II	1.0	1.0	1.3	-	-	1.2	-
Service III	1.0	1.0	0.8	-	-	1.2	-
Service IV	1.0	1.0	-	0.7	-	1.2	-

Source: Author's Analysis, adapted in accordance with SNI 1725:2016

The analyzed configurations consist of two variations of the Aramco CSP bridge. Model 1 represents the Aramco CSP bridge with a 40-meter span, whereas Model 2 represents the Aramco CSP bridge with a 50-meter span. The structural loading configurations for each Aramco CSP bridge model are presented below.

P-ISSN : 2598-1277
E-ISSN : 2621-3966

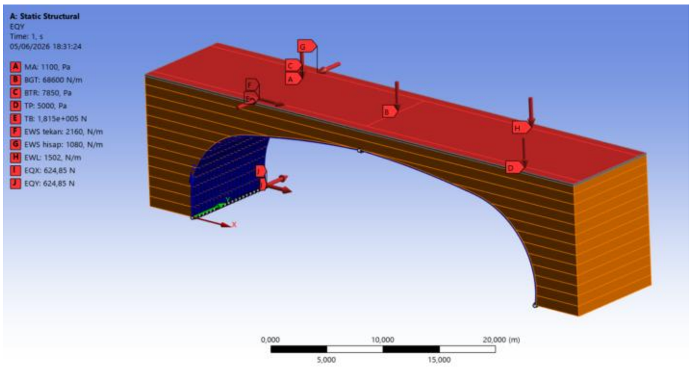

Figure 5. Loading Configuration for Model 1

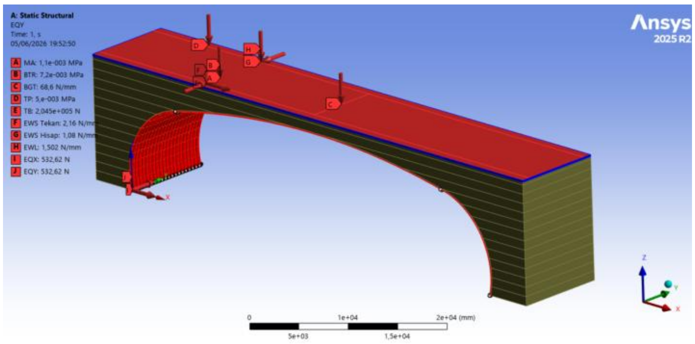

Figure 6. Loading Configuration for Model 2

3. RESULTS AND DISCUSSION

3.1. Total Deformation

Deformation represents the magnitude of displacement of a structural element node from its initial position due to applied structural loads. The total deformation results illustrate the overall extent of deformation experienced by the structure. The total deformation value is determined as the resultant vector of displacements along the X, Y, and Z axes. A lower magnitude of induced deformation indicates a higher structural stiffness in resisting loads. The analytical results for the total deformation of all Aramco CSP bridge models under ultimate and service load combinations are presented in the table below.

Table 4. Recapitulation of Total Deformation Results

Limit State	Model 1 (mm)	Model 2 (mm)
Ultimate		
Strength I	14.405	26.116
Strength II	12.933	23.317
Strength III	7.818	13.568
Strength IV	7.810	13.563
Strength V	7.919	13.792
Extreme Event I	11.444	20.279
Extreme Event II	12.177	21.674
Service		
Service I	11.441	20.487
Service II	12.438	22.350
Service III	10.331	18.866
Service IV	7.687	13.295

Source: Numerical Analysis Results, 2026

 P-ISSN : 2598-1277
E-ISSN : 2621-3966

RSNI T-03-2005, Article 4.7 stipulates that structural deflection evaluations must be conducted utilizing the maximum service load combinations, which encompass live loads alongside dynamic load allowances (impact effects). Consequently, the total deformation results from the Aramco CSP bridge structural analysis are evaluated based on the maximum service limit state load combinations. This evaluation is critical to ensure that the resulting total deformation does not exceed the maximum allowable deflection limits.

Table 5. Maximum Total Deformation Under Service Limit States

Maximum Service Limit State	Deformation (mm)
Model 1 (40-meter Span, SS400)	12.438
Model 2 (50-meter Span, SS490)	22.350

Source: Numerical Analysis Results, 2026

To further elucidate the deformation behavior occurring in each Aramco CSP bridge model, the visual representations of the deformation derived from the finite element method analysis for each model are presented below. These visualizations provide a more comprehensive representation of the structural displacement patterns.

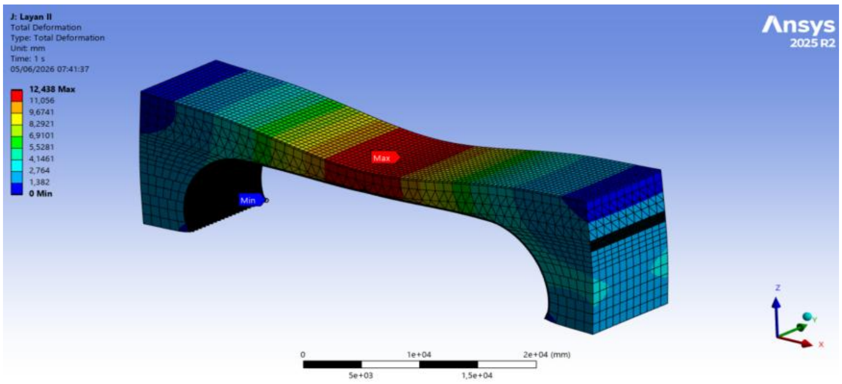

Figure 7. Total Deformation Contour of the Entire Model 1 Structure

Based on Figure 7, it is observed that in Model 1, the maximum deformation occurs at the mid-span of the Aramco CSP structural element (the arch crown), amounting to 12.438 mm. This condition indicates that the load-induced deformation is concentrated at the mid-span, which represents the zone experiencing the maximum bending moment. This deformation profile aligns with the characteristic behavior of arch structures, where the crown area experiences the largest vertical displacement compared to other sections, as illustrated in Figure 8 below.

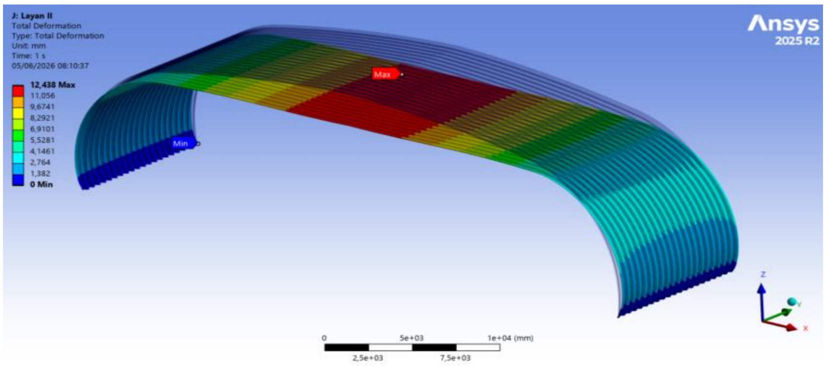

Figure 8. Total Deformation Contour of the Aramco CSP Element in Model 1

P-ISSN : 2598-1277
E-ISSN : 2621-3966

The visual representation of the deformation occurring in Model 2 of the 50-meter span Aramco CSP bridge is presented below to describe the structural deformation behavior under the applied loading conditions.

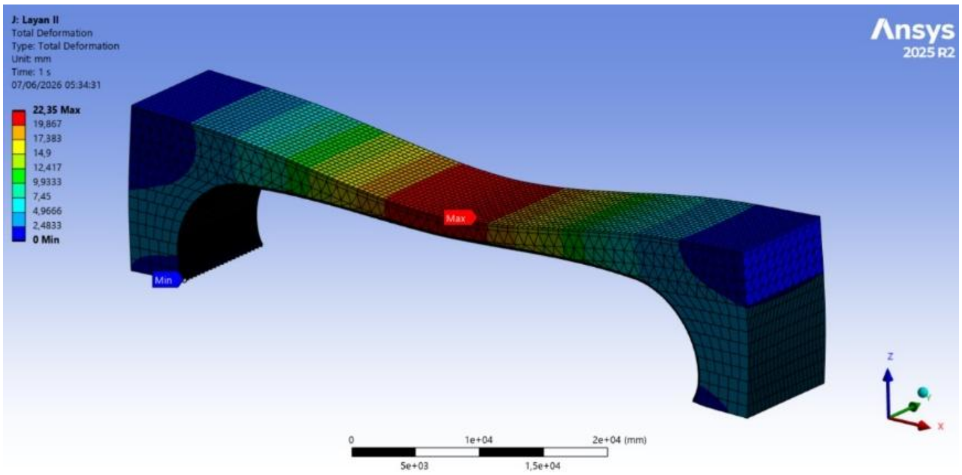

Figure 9. Total Deformation Contour of the Entire Model 2 Structure

Based on Figure 9, it is observed that in Model 2, the maximum deformation occurs at the mid-span of the Aramco CSP structural element (the arch crown), amounting to 22.350 mm. This indicates that the largest load-induced vertical displacement is concentrated at the mid-span area, which represents the most critical zone in resisting bending moment effects. This deformation profile indicates that the structure maintains a reasonable deformation behavior, with a displacement distribution that increases from the supports toward the arch crown, as shown in the following figure.

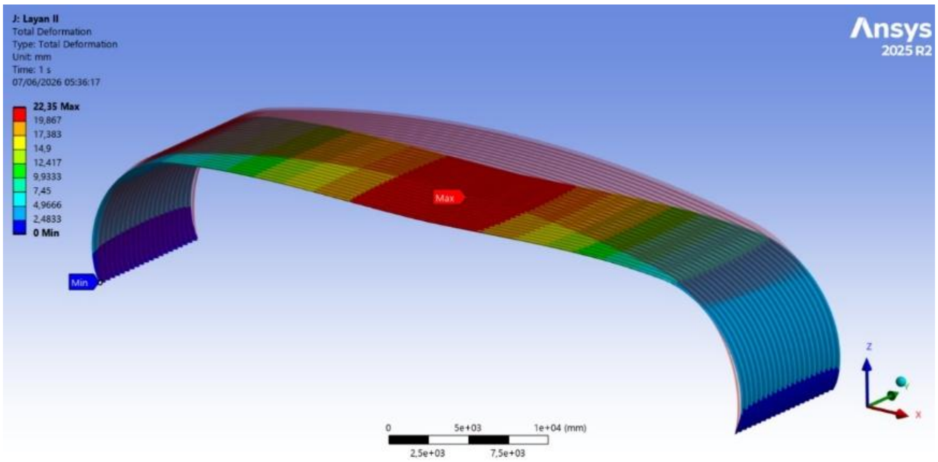

Figure 10. Total Deformation Contour of the Aramco CSP Element in Model 2

In compliance with RSNI T-03-2005, Article 4.7.2, the maximum allowable deflection for simply supported or continuous girders is restricted to 1/800 of the span length. Nevertheless, this provision is fundamentally intended for girder bridge configurations, and to date, no specific standard or regulation explicitly governs the deflection limits for Aramco Corrugated Steel Structure (CSS) bridges. Therefore, this study adopts the aforementioned standard as a conservative baseline to evaluate the induced deformations in accordance with the provisions of RSNI T-03-2005. This criterion serves as an engineering approximation to evaluate the serviceability performance of the Aramco CSP structure.

Table 6. Validation of Total Deformation Against Allowable Limits

Maximum ServiceLimit State	Maximum Deformation (mm)	Allowable Deflection (mm)	Status
Model 1 (40-meter Span, SS400)	12.438	50.000	Compliant
Model 2 (50-meter Span, SS490)	22.350	62.500	Compliant

Source: Author's Analysis, 2026

Table 6 demonstrates that both Aramco CSP bridge configurations—the 40-meter span with a 13 mm CSP thickness and the 50-meter span with a 15 mm CSP thickness—comply with the maximum bridge deflection requirements. Despite the occurrence of deflections, the resulting deformation magnitudes remain well within acceptable thresholds defined by the serviceability criteria. Consequently, the structures preserve their capability to sustain their performance under operational loading conditions.

3.2. Von Mises Equivalent Stress

Von Mises equivalent stress is a combined scalar stress value that represents the actual multi-axial stress state experienced by structural elements under applied loading conditions. Because multiple stress components such as tensile, compressive, and shear stresses can act simultaneously at a specific point or node within a structural element, the Von Mises yield criterion is utilized to simplify these complex stress states into a single equivalent stress value.

Table 7. Recapitulation of Von Mises Equivalent Stress Results

Limit State	Model 1 (MPa)	Model 2 (MPa)
Ultimate		
Strength I	310.33	283.76
Strength II	290.16	263.64
Strength III	222.41	196.02
Strength IV	219.87	193.78
Strength V	222.37	196.36
Extreme Event I	218.21	208.00
Extreme Event II	228.40	218.1
Service		
Service I	270.27	243.78
Service II	283.03	256.35
Service III	257.63	231.35
Service IV	219.06	192.63

Source: Numerical Analysis Results, 2026

The Von Mises equivalent stress results from the Aramco CSP bridge structural analysis are evaluated based on the maximum ultimate limit state load combinations. This evaluation is performed to ensure that the resulting Von Mises equivalent stress magnitudes do not exceed the yield strength thresholds of the Aramco CSP steel material, specifically grade SS400 for Model 1 and grade SS490 for Model 2.

Table 8. Maximum Equivalent Stress Under Maximum Ultimate Limit States

Maximum Ultimate Limit State	Equivalent Stress (MPa)
Model 1 (40-meter Span, SS400)	310.33
Model 2 (50-meter Span, SS490)	283.76

Source: Author's Analysis, 2026

To provide a clear overview of the structural response under operational loads, a stress distribution analysis was conducted on both Aramco CSP bridge models using the finite element method. The

P-ISSN : 2598-1277
E-ISSN : 2621-3966

simulation results, presented as Von Mises stress contours in the following figures, illustrate the stress propagation profiles and identify the locations of stress concentrations in each configuration.

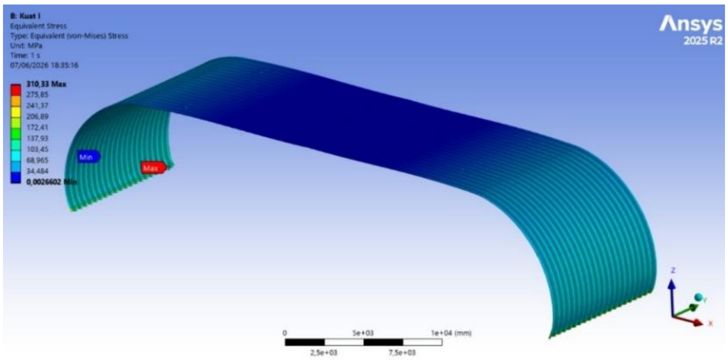

Figure 11. Von Mises Equivalent Stress Contour of Model 1

Based on the FEM analysis results, the induced Von Mises equivalent stress in Model 1 reaches 310.33 MPa. The maximum stress is concentrated at the left-side support area. This region represents the most critical zone as it experiences a combination of axial forces, bending moments, and shear forces transferred from the arch structure to the supports.

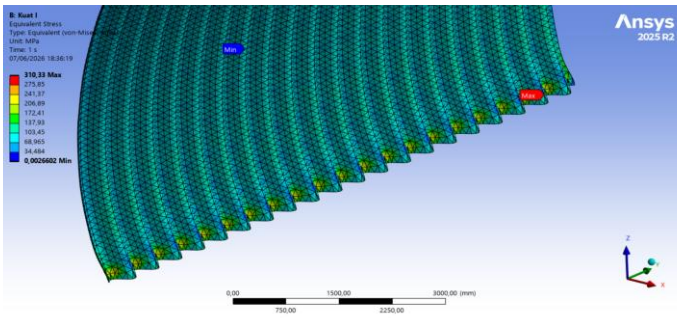

Figure 12. Location of the Maximum Stress Concentration in Model 1

The stress distribution in Model 1 demonstrates that the stress concentration is localized within the Aramco CSP elements adjacent to the supports, subsequently decreasing toward the bridge's arch crown. This profile indicates that the applied loads are gradually transferred from the mid-span toward the supports, thereby rendering the vicinity of the bearings the most critical location with the highest stress response. The visual representation of the Von Mises equivalent stress occurring in Model 2 of the 50-meter span Aramco CSP bridge is presented below to describe the stress behavior under the applied loading conditions.

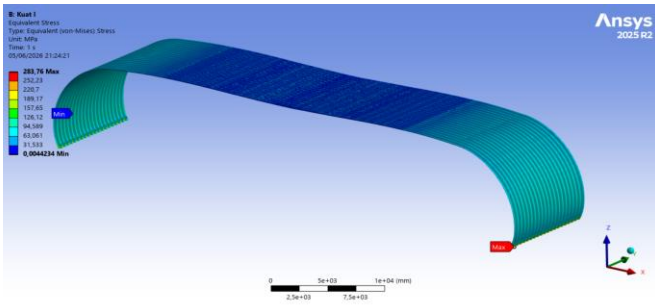

Figure 13. Von Mises Equivalent Stress Contour of Model 2

P-ISSN : 2598-1277
E-ISSN : 2621-3966

The induced Von Mises equivalent stress in Model 2 amounts to 283.76 MPa. This maximum stress occurs at the lower region in the vicinity of the right-side support. The stress concentration at this location indicates that the bearing area acts as the primary load path transferring forces to the foundation. The stress distribution profile shows that the stress magnitudes diminish as the distance from the supports toward the mid-span increases, implying that the load transfer mechanism within the Aramco CSP structure progresses gradually and stably.

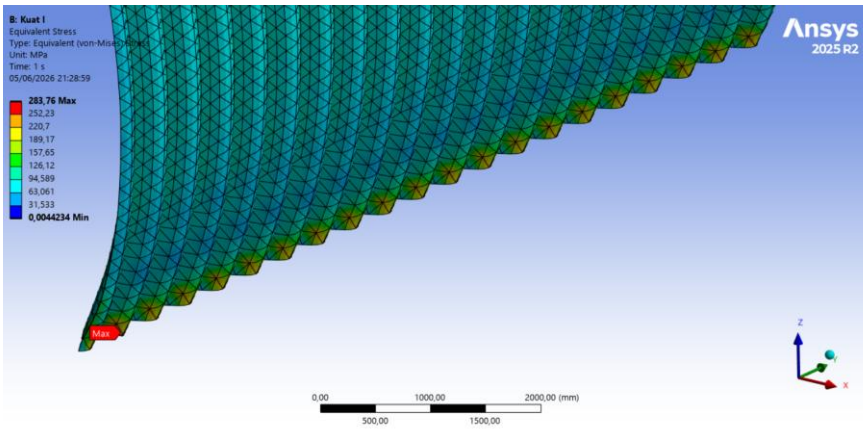

Figure 14. Location of the Maximum Stress Concentration in Model 2

To evaluate structural safety, a validation table comparing the maximum stresses obtained from the numerical analysis against the allowable stress requirements based on the utilized Aramco CSP material grades is presented below.

Table 9. Validation of Von Mises Equivalent Stress Against Allowable Stress Limits

Maximum UltimateLimit State	Maximum Stress (MPa)	Allowable Stress (MPa)	Status
Model 1 (40-meter Span, SS400)	310.33	250.00	Non-compliant
Model 2 (50-meter Span, SS490)	283.76	285.00	Compliant

Source: Author's Analysis, 2026

Model 1 of the Aramco CSP bridge does not satisfy the material's allowable stress requirements. The finite element method (FEM) analysis indicates that the maximum Von Mises equivalent stress of 310.33 MPa exceeds the yield strength of the SS400 steel grade, which is specified at 250 MPa. This structural condition signifies that localized sections of the structural elements have entered the plastic deformation regime, thereby posing a risk of permanent deformation if the operational loading conditions persist. Nonetheless, this maximum stress magnitude remains below the material's ultimate tensile strength, indicating that the structure has not yet reached catastrophic failure. Consequently, design optimization is necessary, such as increasing the corrugated steel plate (CSP) thickness or employing a higher material grade (e.g., SS490), to ensure that the induced stresses remain within the allowable limits. In contrast to Model 1, Model 2 of the Aramco CSP bridge complies with the allowable material stress criteria. The FEM simulation results demonstrate that the maximum equivalent stress of 283.76 MPa remains below the yield strength of the utilized SS490 steel (285 MPa), ensuring that the entire structure operates strictly within the elastic range. This outcome demonstrates that increasing the thickness of the corrugated steel plate (CSP) contributes significantly to enhancing both structural stiffness and cross-sectional capacity. With this superior stiffness, the applied structural loads are distributed more uniformly, effectively mitigating stress concentration zones at critical areas and substantially improving overall structural performance.

P-ISSN : 2598-1277
E-ISSN : 2621-3966

4. CONCLUSION

Based on the finite element structural analysis conducted on the 40-meter and 50-meter span Aramco CSP bridges, the following conclusions are drawn:

1. The 40-meter span Aramco CSP bridge with a 13 mm plate thickness utilizing SS400 steel grade generates a maximum deformation of 12.438 mm, which remains well below the baseline allowable deflection of 50 mm. Similarly, the 50-meter span Aramco CSP bridge with a 15 mm plate thickness utilizing SS490 steel grade experiences a maximum deformation of 22.350 mm, against an allowable deflection limit of 62.5 mm. These findings demonstrate that the maximum induced deformations for both configurations are within the permissible thresholds, indicating that both models satisfy the established structural serviceability requirements.
2. Based on the Von Mises equivalent stress analysis, the 40-meter span Aramco CSP bridge model generates a maximum stress of 310.33 MPa. This magnitude exceeds the 250 MPa yield strength of the SS400 material, signifying that localized plastic deformation occurred at the critical zones of the structure, posing a risk of permanent deformation. Nevertheless, because this maximum stress remains below the material's ultimate tensile strength of 400 MPa, the structure has not reached catastrophic failure. Consequently, design optimization, such as upgrading the material grade or increasing the cross-sectional thickness, is required to mitigate the induced stresses. Conversely, the 50-meter span Aramco CSP bridge model yields a maximum stress of 283.76 MPa, which remains safely below the 285 MPa yield strength of the SS490 steel grade. This confirms that Model 2 operates entirely within the elastic regime, thereby satisfying the strength requirements based on the material's allowable stress criteria.

REFERENCES

[1] B. Kunecki, “Empirical Investigation of the Structural Response of Super-Span Soil–Steel Arches During Backfilling,” *Materials*, vol. 18, no. 15, p. 3650, Aug. 2025, doi: 10.3390/ma18153650.
[2] Z. Wu, F. Liu, Y. Wang, C. Liu, and A. Xu, “Behavior of damaged reinforced concrete arches retrofitted with corrugated stainless steel arches: Experiment, numerical analysis, and calculation method,” *Structures*, vol. 82, p. 110606, Dec. 2025, doi: 10.1016/j.istruc.2025.110606.
[3] C. Machelski and P. Tomala, “Shell Deformation During the Construction of Record Span Soil-steel Buried Structure in Ras-Al-Khaimah (UAE),” *Studia Geotechnica et Mechanica*, vol. 45, no. 3, pp. 197–208, Sep. 2023, doi: 10.2478/sgem-2023-0007.
[4] Y. Zhang, B. Liu, and L. Meng, “Structural behavior and soil arching state of underground corrugated steel utility tunnel,” *J. Constr. Steel Res.*, vol. 203, p. 107798, Apr. 2023, doi: 10.1016/j.jcsr.2023.107798.
[5] T. Maleska and D. Beben, “Behaviour of Soil–Steel Composite Bridges under Strong Seismic Excitation with Various Boundary Conditions,” *Materials*, vol. 16, no. 2, p. 650, Jan. 2023, doi: 10.3390/ma16020650.
[6] K. Lang *et al.*, “Nonlinear analysis of corrugated steel plate culverts using three-dimensional staged modelling under soil–steel interaction,” *Structures*, vol. 79, p. 109480, Sep. 2025, doi: 10.1016/j.istruc.2025.109480.
[7] T. Bensing and M. Moneke, “Development of a novel testing concept for combined characterisation of tensile and compressive properties,” *International Journal of Mechanics and Materials in Design*, vol. 20, no. 5, pp. 895–907, Oct. 2024, doi: 10.1007/s10999-023-09703-3.
[8] A. Wadi, L. Pettersson, and R. Karoumi, “On Predicting the Ultimate Capacity of a Large-Span Soil–Steel Composite Bridge,” *International Journal of Geosynthetics and Ground Engineering*, vol. 6, no. 4, p. 48, Dec. 2020, doi: 10.1007/s40891-020-00232-z.
[9] P. R. T. Naibaho, B. Budiono, A. Surono, and I. Pane, “Studi Eksperimental Perilaku Sambungan Balok-Kolom Eksterior Beton Bubuk Reaktif Terhadap Beban Lateral Siklis,” 2015. Accessed: Jun. 20, 2026. [Online]. Available: https://media.neliti.com/media/publications/145841-ID-studi-eksperimental-perilaku-sambungan-b.pdf

P-ISSN : 2598-1277
E-ISSN : 2621-3966

[10] N. P. A. Yuliadewi, H. Kristijanto, B. Piscesa, P. Suprobo, and F. Aimun, "Shear Buckling Analysis Of Corrugated Web I-Girder With 3D Nonlinear Finite Element Method," *Journal of Civil Engineering*, vol. 36, no. 2, Dec. 2025, doi: 10.12962/j20861206.v36i2.7635.

[11] Rahmawati, B. A. Habsy, and M. Nursalim, "Jenis-Jenis Metode Pengumpulan Data (Qualitative Research)," *Jurnal Pendidikan Tambusai*, pp. 9932–9938, 2025, doi: 10.31004/jptam.v9i1.26166.

[12] H. Putra, "Evaluasi Kekuatan Struktur Baja Bergelombang Berdasarkan Tipe Dan Ketebalan," *Jurnal Jalan Jembatan Direktorat Jendral Bina Marga*, Sep. 2019, Accessed: May 10, 2026. [Online]. Available: https://binamarga.pu.go.id/jurnal/index.php/jurnaljalanjembatan/article/view/908